

Initiation of a superoxide-dependent chain oxidation of lactate dehydrogenase-bound NADH by oxidants of low and high reactivity

FRANK PETRAT, THORSTEN BRAMEY[†], MICHAEL KIRSCH[‡], & HERBERT DE GROOT[¶]

Institut für Physiologische Chemie, Universitätsklinikum, Hufelandstr. 55, D-45122 Essen, Germany

Accepted by Professor M.J. Davies

(Received 7 March 2005; in revised form 16 June 2005)

Abstract

In cells, NADH and NADPH are mainly bound to dehydrogenases such as lactate dehydrogenase (LDH). In cell-free systems, the binary LDH–NADH complex has been demonstrated to produce reactive oxygen species via a chain oxidation of NADH initiated and propagated by superoxide. We studied here whether this chain radical reaction can be initiated by oxidants other than $O_2^{\bullet-}$. LDH largely increased the oxidation of NADH (but not of NADPH) by O_2 , H_2O_2 and during the intermediacy of HNO_2 . LDH also increased the oxidation of NADH by peroxyxynitrite. The increases in NADH oxidation were completely prevented by superoxide dismutase (SOD). In contrast, the nitrogen dioxide-dependent oxidation of NADH and NADPH was decreased by LDH in a SOD-independent manner. These experimental data strongly indicate that oxidation of LDH-bound NADH can be induced from reaction of either weak oxidants with LDH-bound NADH or of strong oxidants with free NADH thus yielding $O_2^{\bullet-}$, which is highly effective to propagate the chain. Our results underline the importance of SOD in terminating superoxide-dependent chain reactions in cells under oxidative stress.

Keywords: *Lactate dehydrogenase, enzyme binding, pyridine nucleotides, oxidants, superoxide, antioxidative capacity*

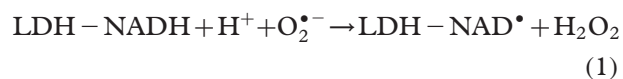
Abbreviations: *SOD, superoxide dismutase; LDH, L-lactate dehydrogenase; carboxy-PTIO, [2-(4-carboxyphenyl)-4,4,5,5-tetramethylimidazole-1-oxyl-3-oxide, Na]; PAPA NONOate, (Z)-1-[N-(3-ammoniopropyl)-N-(n-propyl)amino]diazene-1-ium-1,2-diolate; SIN-1, 3-morpholino-sydnnonimine; DTPA, diethylenetriamine-pentaacetic acid; PCA, principal component analysis; NSC, normalized sensitivity coefficient*

Introduction

Within cells, NADH and NADPH are mainly bound to proteins [1,2], presumably especially to NADH- and NADPH-dependent dehydrogenases. Therefore, lactate dehydrogenase (LDH) is likely to be an important protein for the binding of NADH, due to its high intracellular concentration and affinity for this coenzyme ($K_m = 1.07 \times 10^{-5} \text{ mol l}^{-1}$ [3]). Bielski and Chan [4–9] have demonstrated that the binding to LDH strongly increases the reactivity of NADH towards $O_2^{\bullet-}$ (and the perhydroxyl radical (HO_2^{\bullet})),

which initiates and propagates the oxidation of NADH via a chain radical mechanism, shown in reactions (1)–(4).

Initiation:



Propagation:

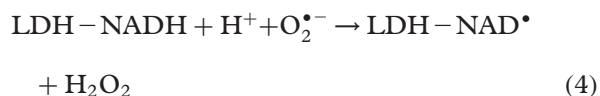


Correspondence: F. Petrat, Institut für Physiologische Chemie, Universitätsklinikum, Hufelandstr. 55, D-45122 Essen, Germany.
Tel: 49 201 723 4105. Fax: 49 201 723 5943. E-mail: frank.petrat@uni-essen.de

[†] Tel: 49 201 723 4111. E-mail: thorsten.bramey@uni-essen.de

[‡] Tel: 49 201 723 4108. E-mail: michael.kirsch@uni-essen.de

[¶] Tel: 49 201 723 4101. E-mail: h.de.groot@uni-essen.de



These findings suggest that NADH in the presence of LDH exhibits prooxidative capabilities—in contrast to its proposed antioxidative capacity [10–12]—since the initiating $\text{O}_2^{\bullet -}$ is regenerated and one H_2O_2 molecule is formed per initiation (reaction (1)) and one per propagation chain cycle (reactions (2)–(4)). However, reactions between LDH-bound NADH and oxidants other than $\text{O}_2^{\bullet -}$ (HO_2^{\bullet}) have not been reported so far. Therefore, our aim here was to study the effects of LDH on the reactivity of NADH and NADPH towards a variety of weak (O_2 , H_2O_2 , HNO_2) as well as strong oxidants (peroxynitrite and NO_2^{\bullet}) and to find out whether these oxidants are capable of initiating a prooxidative chain radical reaction propagated by $\text{O}_2^{\bullet -}$.

Materials and methods

Materials

L-lactate dehydrogenase (LDH) from hog muscle (EC 1.1.1.28), superoxide dismutase (SOD) from bovine erythrocytes (EC 1.15.1.1), NADH and NADPH were purchased from Roche Molecular Biochemicals (Mannheim, Germany). Chelex 100, diethylenetriamine-pentaacetic acid (DTPA), oxamate, H_2O_2 , manganese dioxide and isoamyl nitrite were obtained from Sigma (Deisenhofen, Germany). KH_2PO_4 , K_2HPO_4 , NaNO_2 and n-hexane were from Merck (Darmstadt, Germany). The specific NO^{\bullet} -oxidant [2-(4-carboxyphenyl)-4,4,5,5-tetramethylimidazole-1-oxyl-3-oxide, Na] (carboxy-PTIO) was obtained from Calbiochem (Darmstadt) and (Z)-1-[N-(3-ammoniopropyl)-N-(n-propyl)amino]diazene-1-ium-1,2-diolate (PAPA NONOate) was from Situs (Düsseldorf, Germany). The peroxynitrite generator 3-morpholinopyridone (SIN-1) was generously provided by Drs K. Schönafinger and J. Pünter (Aventis, Frankfurt/Main, Germany). Oxoperoxynitrate(1-) (ONOO^-) was prepared by isoamyl nitrite-induced nitrosation of hydrogen peroxide (0.12 mol isoamyl nitrite, 100 ml H_2O_2 (1 M) plus the transition metal chelator DTPA (2 mM)), purified (i.e. solvent extraction, removal of excess H_2O_2 , N_2 -purging) as described by Uppu and Pryor [13] and stored at -79°C . All other chemicals were of the highest purity commercially available. Solutions were prepared using water received from a TKA-LAB purification system (Niederelbert, Germany, type HP 6 UV/UF).

Determination of the binding stoichiometries of LDH and NADH or NADPH

The binding stoichiometries of NADH or NADPH and LDH under the applied experimental conditions were determined by ultracentrifugation according to [14]. LDH (0.1–4.2 μM) was incubated with 4.2 μM NADH or NADPH in phosphate buffer (50 mM $\text{KH}_2\text{PO}_4/\text{K}_2\text{HPO}_4$, pH 7.5, 25°C). Then samples were taken and the enzyme activity determined photometrically according to Bergmeyer [15]. Additionally, fluorescence spectra of NADH and NADPH ($\lambda_{\text{exc.}} = 340 \text{ nm}$; $\lambda_{\text{em.}} = 400\text{--}600 \text{ nm}$) were scanned with a spectrofluorometer (Shimadzu, Duisburg, Germany; type RF-1501). Afterwards, samples were centrifuged (371,000g, 25°C , 5 h) using an ultracentrifuge (Beckman Coulter, Krefeld, Germany; type Optima™ L-70k, Rotortype 70 Ti). Then again, enzyme activity was determined and fluorescence spectra of NADH and NADPH were recorded from both the supernatant and the pellet (subsequent to resuspension of the latter). The amount of NADH or NADPH bound to the enzyme was quantified from the decrease in the fluorescence intensity of NADH or NADPH within the supernatant subsequent to centrifugation compared to LDH-free solutions of NADH or NADPH. The binding stoichiometry of LDH and NADH or NADPH was calculated based on the concentration of LDH-bound NADH or NADPH in relation to the enzyme concentration.

Assessment of the influence of LDH on the fluorescence of NADH or NADPH

The effect of LDH on the fluorescence intensity of NADH or NADPH (4.2 μM) was assessed from fluorescence spectra ($\lambda_{\text{exc.}} = 340 \text{ nm}$, $\lambda_{\text{em.}} = 400\text{--}600 \text{ nm}$) of the pyridine nucleotides in the absence and presence of the enzyme (2.1 μM , in phosphate buffer, pH 7.5, 25°C).

Determination of the effect of peroxynitrite on the oxidation of NADH or NADPH in the absence and presence of LDH

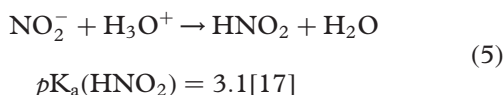
Phosphate buffer (pH 7.5, 25°C) with or without LDH (5–20 μM) was supplemented with NADH or NADPH (150 μM , each) and transferred to reaction tubes (Eppendorf, Hamburg, Germany). Then ONOO^- (100–280 μM) was added, using the drop-tube Vortex mixer technique as described previously [16]. Oxidation of NADH or NADPH was photometrically assessed from the decrease in the optical density at 340 nm (UV mini 1240, Shimadzu, Duisburg, Germany). In some experiments SOD (20–50 U ml^{-1}) was added and/or the catalytic centers of LDH were blocked by addition of the inhibitor oxamate (1 mM) prior to the addition of peroxynitrite.

Experiments with the peroxy-nitrite generator 3-morpholino-sydnonimine (SIN-1) were performed under the same experimental conditions as described above for authentic peroxy-nitrite. SIN-1 (1 mM) was added to phosphate buffer (pH 7.5, 25°C) containing NADH or NADPH (150 μM) and DTPA (100 μM) in the absence and presence of LDH (10 μM). Oxidation of NADH or NADPH was assessed by continuous UV/visible spectrophotometric recordings of the absorption at 340 nm (UV/Visible Lambda 40, PerkinElmer Life Sciences, Norwalk, CT, USA). Further experiments were performed in the absence and presence of oxamate (1 mM) and SOD (20–50 U ml⁻¹), respectively.

Assessment of the effect of O₂, H₂O₂, HNO₂ and NO₂[•] on the oxidation of NADH or NADPH in the absence and presence of LDH

The effect of LDH (10 μM) on the (auto)oxidation of NADH or NADPH (150 μM) by molecular oxygen was studied in phosphate buffer (pH 7.0, 25°C) containing the transition metal chelator DTPA (100 μM) under ambient atmosphere (i.e. at ≈ 225 μM O₂). The oxidizing effect of H₂O₂ (600 μM) was determined under the same experimental conditions.

HNO₂ was generated from nitrite (NO₂⁻, added as NaNO₂, 10 mM), as shown in reaction 5. The experiments were performed in phosphate buffer (37°C) at pH 7.0—in order to stimulate the formation of HNO₂ [17]—containing NADH or NADPH (150 μM) in the absence and presence of LDH (10 μM) and SOD (50 U ml⁻¹), respectively.



A kinetical simulation performed with the full reaction set outlined in [18] predicted that only HNO₂ is formed at substantial concentrations during a reaction time of 120 min (equilibrium concentrations: HNO₂ (1.25 μM), NO₂[•] (0.1–0.8 nM), N₂O₃ (0.15 pM), and N₂O₄ (0.02–0.15 pM)).

The NO₂[•] radical was generated from the NO[•] donating compound PAPA NONOate (100 μM) and increasing concentrations of carboxy-PTIO (5–100 μM) under ambient atmosphere [19] in Chelex 100-treated [20] phosphate buffer (pH 7.5, 37°C) containing NADH or NADPH (150 μM) as a target in the absence and presence of LDH (10 μM). In some experiments SOD (50 U ml⁻¹) was added to the buffer prior to the addition of PAPA NONOate and carboxy-PTIO. Oxidation of NADH or NADPH was recorded by monitoring its UV/visible absorption at 340 nm using phosphate buffer as blank.

Kinetic simulations of oxidant-dependent consumption of NADH or NADPH

Kinetic simulations were performed with the KINTECUS V3.7 program written by Dr James C. Ianni (www.kintecus.com). The kinetic model and the complete reaction set of 118 reactions of reactive oxygen and nitrogen oxide species as described in Kirsch et al. [18] was supplemented with 20 reactions outlined in Table I in order to simulate the oxidation of NADH under the various experimental conditions. To determine the reactions of interest in a ranked order, sensitivity analyses [21] were performed for some simulations. For this purpose, the normalized sensitivity coefficients (NSCs) were calculated by the KINTECUS program:

$$\text{NSC} = \frac{\delta \ln [\text{species}]}{\delta \ln k}$$

The NSCs were analyzed by means of principal component analysis (PCA) at 80 time points according to Vajjda et al. [22] with the aid of the ATROPOS program, which was additionally written by Ianni (see above). The ATROPOS software eliminates with a PCA superfluous, redundant chemical steps and ranks the resulting chemical steps by calculating the corresponding overall sensitivity coefficients (B_r).

Statistics

All experiments were performed in duplicate and repeated at least twice. Traces shown in the figures are representative of all the corresponding experiments performed. The data are expressed as means ± S.D.

Results

Binding stoichiometry of LDH and NADH or NADPH

Determination of the binding stoichiometries of NADH and LDH under the experimental conditions applied here confirmed, in line with previous studies [23,24], that LDH binds four NADH molecules, i.e. one NADH molecule per subunit of the enzyme, when the coenzyme concentration exceeds the concentration of the enzyme 40-fold (data not shown). As expected, NADPH was hardly bound, even when it was applied in excess.

Effect of LDH on the fluorescence of NADH or NADPH

In previous studies it has been demonstrated that the binding to proteins can result in an increased fluorescence intensity of pyridine nucleotides [1,25–27] and it has been suggested that these increases reflect changes in the conformation and/or the redox capabilities of the coenzymes [2,26]. Changes in the conformation of NADH as induced by LDH have

Table I. Subset of relevant reactions and rate constants used in the kinetic simulation of NADH oxidation in the absence and presence of LDH.

Entry	Reaction	k [$M^{-1}s^{-1}$]*	References	k_{app} [$M^{-1}s^{-1}$]*	Remarks
1	$NADH + O_2 \rightarrow NAD^+ + H_2O_2$	6.8×10^{-10}	[43]		Assuming $[O_2] = 225 \mu M$
2	$NADH + H_3O^+ \rightarrow HNADH^+ + H_2O$	7			$k_2 = 5.6 \times 10^{-5} s^{-1}$ at pH 5.1 and $k_2 = 5.9 \times 10^{-4} s^{-1}$ at pH 4.1 [44]
3	$LDH-NADH + O_2 \rightarrow LDH-NAD^{\bullet} + H^+ + O_2^{\bullet-}$			1.6×10^{-4}	This paper; assuming $[O_2] = 225 \mu M$
4	$NADH + O_2^{\bullet-} \rightarrow NAD^{\bullet} + HOO^-$	2.7	[5]		$k_4 \ll 27 M^{-1} s^{-1}$ [45]
5	$LDH-NADH + O_2^{\bullet-} \rightarrow LDH-NAD^{\bullet} + HOO^-$	3.6×10^4			Extracted from data given in [28]
6	$NADH + H_2O_2 \rightarrow NAD^+ + H_2O + HO^-$	3.5×10^{-5}		2.0×10^{-4}	This paper
7	$LDH-NADH + H_2O_2 \rightarrow$ product that yields $O_2^{\bullet-}$				
8	$NADH + HO_2^{\bullet} \rightarrow NAD^{\bullet} + H_2O_2$	1.8×10^5	[6]		
9	$LDH-NADH + HO_2^{\bullet} \rightarrow LDH-NAD^{\bullet} + H_2O_2$	2.0×10^6	[6]		
10	$NADH + ONOOH \rightarrow NAD^{\bullet} + H_2O + NO_2$	7.4×10^3	[36]		
11	$NADH + O_2NOOH \rightarrow NAD^{\bullet} + H_2O_2 + NO_2^{\bullet-}$	1.0×10^4	[46]		
12	$LDH-NADH + HNO_2 \rightarrow LDH-NAD^{\bullet} + NO^{\bullet} + H_2O$			520	This paper
13	$NADH + NO_2^{\bullet} \rightarrow NAD^{\bullet} + HNO_2$	4.0×10^3			
14	$LDH + NADH \rightarrow LDH-NADH$	1.0×10^6	[35]		Estimated
15	$LDH-NADH \rightarrow LDH + NADH$	1.0×10^1			From entry 14 and $K_m = 1.07 \times 10^{-5}$ [3]
16	$LDH + NAD^{\bullet} \rightarrow LDH-NAD^{\bullet}$	1.0×10^6			Estimated
17	$LDH-NAD^{\bullet} \rightarrow LDH + NAD^{\bullet}$	2.5×10^2			From entry 16 and $K_m = 2.53 \times 10^{-4}$ [3]
18	$NAD^{\bullet} + O_2 \rightarrow NAD^+ + O_2^{\bullet-}$	2.0×10^9	[45]		
19	$LDH-NAD^{\bullet} + O_2 \rightarrow LDH-NAD^+ + O_2^{\bullet-}$	3.2×10^9	[6]		
20	$2 NAD^{\bullet} \rightarrow (NAD)_2$	5.6×10^7	[5]		

k_{app} : optimized apparent rate constants. * At ambient temperature (25°C) or 37°C (entries 12 and 13).

Note: This subset of reactions and rate constants was included in the simulation of the reactions of reactive oxygen and nitrogen oxide species as given in Ref. [18]. Simulating parameters see Legends to Table I–III.

been proposed [4] to be responsible for an enhanced reactivity of NADH towards $O_2^{\bullet-}$ (HO_2^{\bullet} [4–7]).

In samples containing LDH (2.1 μM) we determined a 2-fold increase in fluorescence intensity ($\lambda_{\text{exc.}} = 340 \text{ nm}$, $\lambda_{\text{em.}} = 460 \text{ nm}$) of NADH (4.2 μM), whereas NADPH fluorescence was not altered (data not shown). Therefore, the increase in NADH fluorescence intensity observed here was expected to reflect an increased reactivity of the coenzyme towards oxidants, whereas no changes in the reactivity of NADPH, which hardly bound to LDH, were expected.

Effect of LDH on the oxidation of NADH or NADPH induced by oxygen and hydrogen peroxide in the absence and presence of SOD

In the absence of LDH, NADH (150 μM) was rather stable in phosphate buffer (pH 7.0, 25°C) under normoxic conditions, i.e. only $3.9 \pm 4.2 \mu\text{M}$ NADH were oxidized during 2 h of incubation in the presence of $\approx 225 \mu\text{M}$ O_2 (Figure 1a). In samples containing LDH (10 μM), however, NADH was oxidized about 5-fold faster. In contrast to NADH, the enzyme had almost no enhancing effect on the oxidation of NADPH (data not shown). The enhanced oxidation of NADH in the presence of LDH was almost completely prevented by SOD (50 U ml^{-1} ; data not shown).

Bernofsky and Wanda [28] have demonstrated that H_2O_2 , known to be ubiquitously present in aqueous solutions, slowly oxidizes NADH yielding NAD^+ , H_2O and HO^- , and a rate constant of $3.5 \times 10^{-5} \text{ M}^{-1} \text{ s}^{-1}$ can be extracted from their work (Table I, entry 6). In line with this, H_2O_2 (600 μM) only slightly oxidized NADH in the absence of LDH (Figure 1b). The presence of LDH (10 μM) significantly accelerated the oxidation of NADH. SOD (50 U ml^{-1}) again completely counteracted the LDH-dependent oxidation of NADH (data not shown). In contrast to NADH, the oxidation of NADPH was hardly increased by the enzyme (data not shown).

The finding that in both examples, SOD (almost) completely inhibited oxidation of LDH-bound NADH clearly indicates that the major amount of NADH was obviously oxidized by $O_2^{\bullet-}$. This behavior is in accordance with a chain radical mechanism where the chain is initiated by O_2 or H_2O_2 and propagated by $O_2^{\bullet-}$ according to reactions (1)–(4). In order to provide further evidence for the chain mechanism characterized above, kinetic simulations were performed. To take into consideration all known initiation, propagation and termination reactions, we applied our established reaction set for reactive oxygen and nitrogen oxide species [18] which was further extended with the 20 reactions given in Table I. The simulations fitted the experimental data in a satisfactory manner (Figure 1) when slow initiation reactions

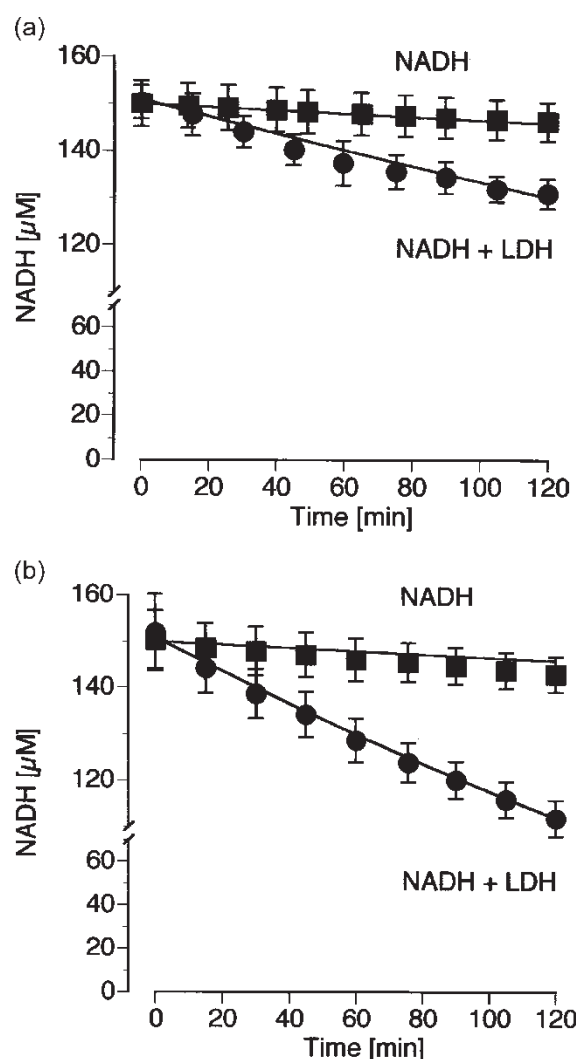


Figure 1. Effect of LDH on the oxidation of NADH induced by molecular oxygen and H_2O_2 . NADH (150 μM) was incubated with or without lactate dehydrogenase (LDH, 10 μM) in phosphate buffer (50 mM, pH 7.0, 25°C) containing the transition metal chelator diethylenetriamine-pentaacetic acid (100 μM). (a), (auto)oxidation of NADH in the absence and presence of LDH under normoxic conditions. (b), effect of LDH on NADH oxidation induced by H_2O_2 (600 μM). NADH oxidation was assessed by spectrophotometric recordings of the decrease in NADH absorption at 340 nm. Data shown are means \pm S.D. of two independent experiments. The lines shown are the predictions of the kinetic simulations performed with the combined reaction set given in Ref. [18] and in Table I.

($k \approx 2 \times 10^{-4} \text{ M}^{-1} \text{ s}^{-1}$) between O_2 or H_2O_2 and LDH-bound NADH were respected (Table I, entries 3 and 7). These initiation reactions presumably involve single electron transfer from enzyme-bound NADH to the oxidants, comparable to the (weak and unspecific) NADH- and NADPH-oxidase activities known for other enzymes (e.g. flavoenzymes [29]). To obtain a clearer picture which reactions of our full kinetic scheme (138 reactions) would have the strongest influence, a sensitivity analysis was carried out including PCA of the sensitivity matrix.

The subsequent performed analysis of the PCA with the ATROPOS software reduced the full kinetic scheme to 23 and 18 reactions, respectively, (Tables IS and IIS) and ranked these reactions due to their importance. As expected, the reaction of O_2 with LDH–NADH (Table I, reaction (3)) is most important for the LDH-enhanced autoxidation of NADH but of minor importance when NADH is oxidized in the presence of LDH and H_2O_2 . However, in both cases the $O_2^{\bullet-}$ -dependent propagation reaction (4) is predicted to be a dominant reaction channel, as was already verified by the strong influence of SOD in these systems.

Effect of LDH on the oxidation of NADH or NADPH induced by SIN-1 and peroxyntirite in the absence and presence of SOD

SIN-1, an intermediate of the pro-drug molsidomine, is often used in experimental systems for the *in situ* generation of stoichiometric amounts of peroxyntirite [11,30,31]. In aqueous solutions, SIN-1 decays at neutral pH ($t_{1/2} = 40$ min [32]) forming SIN-1A [33] which, in the presence of O_2 , spontaneously fragments to yield SIN-1C, nitric oxide (NO^*), and $O_2^{\bullet-}$, respectively. Peroxyntirite is formed by recombination of these radicals in a diffusion-controlled reaction ($k = 6.7 \times 10^9 M^{-1} s^{-1}$ [34]).

SIN-1 (1 mM) already oxidized NADH and NADPH (150 μM , each) in the absence of LDH at a considerable rate (Figure 2a; compare with Figures 1a/b). LDH (10 μM) further enhanced the SIN-1-dependent oxidation of NADH about 7-fold. In contrast to NADH, the SIN-1-mediated oxidation of NADPH was even slightly hampered by the enzyme. Since 10 μM LDH—binding 28 μM NADH under these conditions—mediated the oxidation of 105 μM NADH (within the first 20 min), the LDH-bound coenzyme was obviously exchanged about four times subsequent to its oxidation. SOD (50 U ml^{-1}) almost completely prevented the SIN-1-induced oxidation of NADH, both in the presence and in the absence of LDH (Figure 2b). The strong inhibitory effect of SOD most likely resulted from scavenging of $O_2^{\bullet-}$ directly released from SIN-1—and thus from the decreased formation of peroxyntirite—as well as from scavenging of $O_2^{\bullet-}$ resulting from the reaction of the remaining peroxyntirite with free NADH [11,35–37]. Thus, SOD prevented the initiation reaction, i.e. the $O_2^{\bullet-}$ -yielding attack of peroxyntirite on free NADH, and terminated the propagation reaction via superoxide.

In order to clarify whether the binding of NADH to the substrate binding site of LDH is a prerequisite for the LDH-enhanced oxidation of NADH, experiments were performed in the presence of the inhibitory substrate analogue oxamate (1 mM [23,25]). Oxamate, in combination with NADH

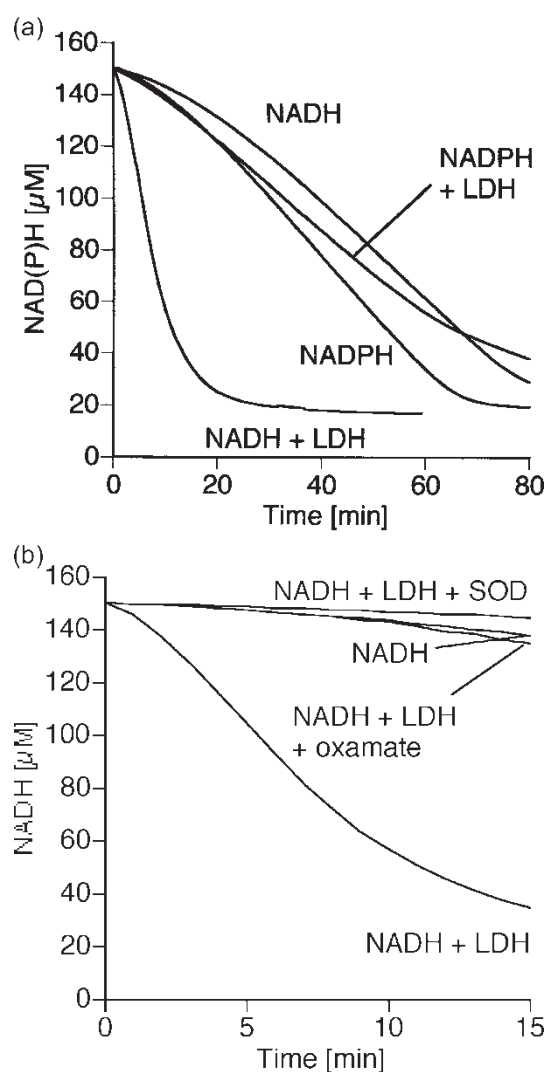


Figure 2. Effect of LDH on the oxidation of NADH or NADPH induced by SIN-1. (a), NADH or NADPH (150 μM) was incubated in the absence and presence of lactate dehydrogenase (LDH, 10 μM) in phosphate buffer (50 mM, pH 7.5, 25°C) containing the transition metal chelator diethylenetriamine-pentaacetic acid (100 μM) and the peroxyntirite generator 3-morpholino-sydnonimine (SIN-1, 1 mM). (b), effect of superoxide dismutase (SOD, 50 U ml^{-1}) and the LDH inhibitor oxamate (1 mM) on the oxidation of NADH induced by SIN-1; the other experimental conditions were the same as in (a). Oxidation of NADH or NADPH was assessed by spectrophotometric recordings of the decrease in absorption at 340 nm. Traces shown are representative of two independent experiments.

has been reported to close off the active site of the LDH-subunits [23], so that NADH bound to the active site would be no longer accessible for oxidants. In line with these considerations, the enhancing effect of LDH on the oxidation of NADH was completely abolished in the presence of oxamate (Figure 2b). Free NADH and NADPH were only slightly protected by the inhibitor (data not shown), indicating that oxamate does not effectively scavenge peroxyntirite and other reactive species released from SIN-1.

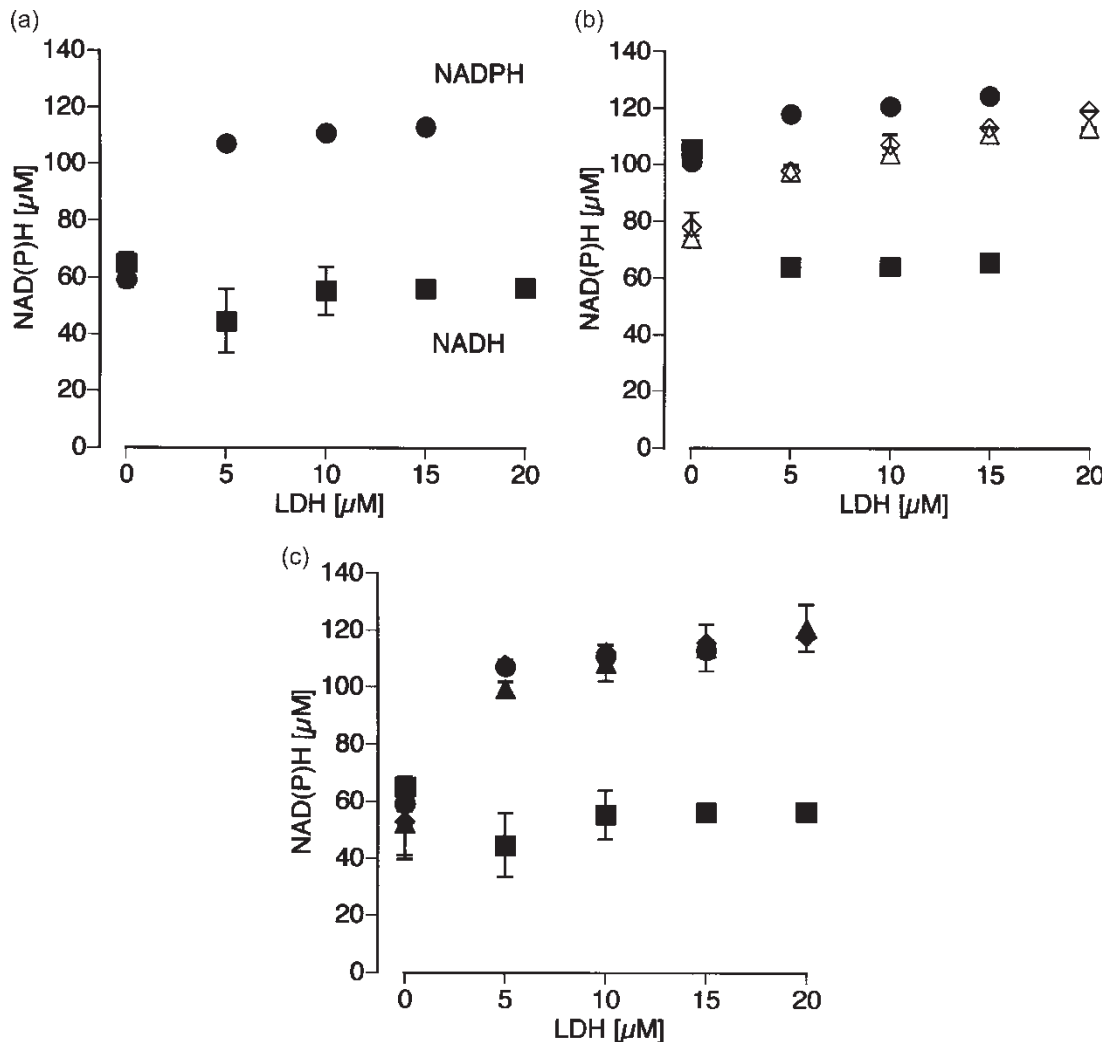


Figure 3. Effect of LDH on the oxidation of NADH or NADPH induced by authentic peroxyntirite. NADH or NADPH (150 μM) was incubated with or without lactate dehydrogenase (LDH, 5–20 μM) in phosphate buffer (50 mM, pH 7.5, 25°C). (a), effect of LDH on the oxidation of NADH or NADPH induced by authentic peroxyntirite (280 μM) as added using the drop-tube Vortex mixer technique (see text). (b), effect of superoxide dismutase (SOD, 50 U ml⁻¹) on the oxidation of NADH or NADPH induced by peroxyntirite (100 μM) in the absence and presence of LDH. (c), effect of the competitive LDH inhibitor oxamate (1 mM) on the oxidation of NADH or NADPH induced by peroxyntirite (280 μM) in the absence and presence of LDH; the experimental conditions in (b) and (c) were the same as in (a). Oxidation of NADH or NADPH was photometrically assessed 5 min after addition of peroxyntirite from the decrease in absorption at 340 nm; prolonged incubation led to no further oxidation of NADH or NADPH by peroxyntirite. Values shown represent means ± S.D. of two independent experiments (S.D.s not visible are hidden by the symbols); square = LDH + NADH, circle = LDH + NADPH, open triangle = LDH + NADH + SOD, open rhombus = LDH + NADPH + SOD, solid triangle = LDH + NADH + oxamate, solid rhombus = LDH + NADPH + oxamate.

To study the effect of peroxyntirite directly, experiments with authentic peroxyntirite were performed. As already found in experiments with SIN-1, the oxidation of NADH in the presence of LDH was again increased, but to a much lesser extent (Figure 3a). Surprisingly, when NADH was replaced by NADPH, LDH (10 μM) diminished the peroxyntirite-dependent oxidation of the reduced nicotinamide by almost 60%. Since equal amounts of NADH and NADPH were oxidized by peroxyntirite in the absence of LDH, the true enhancement of NADH oxidation by the enzyme is given by comparison with the experiments performed with LDH and NADPH,

demonstrating that LDH mediated a more than 2-fold increase in peroxyntirite-induced NADH oxidation. In the presence of SOD (50 U ml⁻¹) the same amounts of NADH and NADPH were oxidized by peroxyntirite (Figure 3b), indicating that the LDH-dependent increase in NADH oxidation was propagated again by superoxide. Similar results as described for SOD were obtained with oxamate (Figure 3c).

The effect of SOD again suggests that in these experiments the enhanced NADH oxidation mediated by LDH results from a free radical chain mechanism propagated by O₂^{•-}. This contrasts, however, to recent experiments where we found that the reaction of

peroxynitrite with NADH yields surprisingly low amounts of both superoxide and H_2O_2 [36], although freely diffusing NADH and NADPH was oxidized to a significant extent by peroxynitrite, i.e. effective formation of $\text{O}_2^{\bullet-}$ via reduction of O_2 by NAD^{\bullet} had to be expected. An explanation for this apparent discrepancy is obviously an effective scavenging of NO_2^{\bullet} by LDH. The attack of peroxynitrite on NADH yields the intermediates $\text{O}_2^{\bullet-}$ and NO_2^{\bullet} [11,37]. Both radicals readily recombine in a diffusion-controlled reaction yielding peroxynitrate (O_2NOO^-), which is unable to oxidize NADH at physiological pH [37]. Due to the high concentration of LDH ($10\ \mu\text{M}$) as compared to the $\text{O}_2^{\bullet-}$ equilibrium concentration ($0.02\ \mu\text{M}$, according to the kinetic simulation), the enzyme can compete with $\text{O}_2^{\bullet-}$ for NO_2^{\bullet} . Given that one LDH molecule contains 42 tyrosine residues [38] and that one peptide-bound tyrosine reacts with NO_2^{\bullet} at a rate constant of $3.2 \times 10^5\ \text{M}^{-1}\text{s}^{-1}$ [39], the rate constant thus estimated for the reaction of LDH with NO_2^{\bullet} would be $1.3 \times 10^7\ \text{M}^{-1}\text{s}^{-1}$. The relative amount of LDH-trapped NO_2^{\bullet} can then be estimated as $(10\ \mu\text{M} \times 1.3 \times 10^7\ \text{M}^{-1}\text{s}^{-1}) / (0.02\ \mu\text{M} \times 4.5 \times 10^9\ \text{M}^{-1}\text{s}^{-1}) = 1.5/1$. Thus, about 67% of the nitrogen dioxide is expected to be trapped by LDH in this reaction, so that the thus increased $\text{O}_2^{\bullet-}$ equilibrium concentration is sufficient to initiate and propagate the chain reaction of LDH-bound NADH (reactions (1)–(4)). These considerations neglect that not each tyrosine residue is accessible to NO_2^{\bullet} . However, on the other hand, other amino acid residues such as tryptophanyl and cysteinyl residues should react with NO_2^{\bullet} as well.

In the absence of LDH, the yield of the peroxynitrite-dependent ($100\ \mu\text{M}$) formation of NAD^+ (i.e. $43.2 \pm 2.0\ \mu\text{M}$) was satisfactorily predicted by our kinetical simulation ($41.3\ \mu\text{M}$). The PCA reduced the full kinetic scheme to 44 reactions (Table IIIS) and predicted that the freely diffusing nucleotides were mainly oxidized by peroxynitrous acid ($B_r = 6514.3$) and only to a minor extent by the radicals derived from it, which is in line with our previous finding [36]. In the presence of LDH, however, we were not capable of simulating the results obtained with either SIN-1 or authentic peroxynitrite. We presumed that this failure was due to the scavenging activity of LDH in these reactions as indicated by the decreased NADPH oxidation in the presence of the enzyme, which was especially pronounced in the experiments with authentic peroxynitrite (Figure 3a). Effective scavenging of the chain radical initiating entities (e.g. ONOOH , HO^{\bullet} , NO_2^{\bullet}) by LDH may also account for the rather low increase in NADH oxidation mediated by LDH in the presence of authentic peroxynitrite as compared to *in situ*-generated peroxynitrite (SIN-1). The possibility that $\text{O}_2^{\bullet-}$ as released during SIN-1 decay decisively oxidized LDH-bound NADH is

rather unlikely, because SIN-1 additionally releases NO^{\bullet} that combines with $\text{O}_2^{\bullet-}$ to yield peroxynitrite in a diffusion-controlled reaction ($k = 6.7 \times 10^9\ \text{M}^{-1}\text{s}^{-1}$ [34]), whereas the rate constant of LDH-bound NADH with $\text{O}_2^{\bullet-}$ is about 2×10^5 -fold lower (Table I, entry 5). Keeping in mind that under the conditions given above $28\ \mu\text{M}$ NADH are bound to LDH, one can calculate that NO^{\bullet} at subnanomolar concentrations, i.e. $[\text{NO}^{\bullet}] = [\text{LDH-NADH}] \times 3.6 \times 10^4 / (6.7 \times 10^9) = 0.15\ \text{nM}$, can compete with LDH-NADH for $\text{O}_2^{\bullet-}$. Therefore, the remaining amounts of superoxide from SIN-1, i.e. $\leq 0.15\ \text{nM}$, are too low to effectively support the propagation reaction (reaction (4)), whereas substantially higher amounts of superoxide are generated from the reaction of NADH with peroxynitrite.

Effect of LDH on the oxidation of NADH or NADPH induced by HNO_2 and NO_2^{\bullet} in the absence and presence of SOD

The experiments performed to this point clearly indicate that a small part of NADH bound to LDH is oxidized by the initiation reactions with weak oxidants but that the major part of LDH-bound NADH is oxidized by $\text{O}_2^{\bullet-}$ during propagation of the free radical chain. There was no evidence that strong oxidants such as ONOOH oxidized LDH-bound NADH directly, presumably because they readily react with the protein moiety of the enzyme before getting access to the coenzyme bound at the active site. To further support these assumptions, we performed additional experiments with the weak oxidant HNO_2 on the one hand, and with the strong oxidant NO_2^{\bullet} , on the other.

When $10\ \text{mM}$ sodium nitrite was added at pH 7.0 in the absence of LDH, NADH was very slowly oxidized in a linear manner (Figure 4a). LDH ($10\ \mu\text{M}$) strongly accelerated the HNO_2 -dependent oxidation of NADH (Figure 4a). As in experiments with O_2 and H_2O_2 , NADPH was not significantly faster consumed in the presence of LDH and the enzyme failed to protect the pyridine nucleotide against the attack of HNO_2 , indicating that LDH does not effectively react with this oxidant (data not shown). The enhanced NADH oxidation in the presence of LDH could be completely prevented by SOD ($50\ \text{U ml}^{-1}$, data not shown).

In the presence of LDH the time dependence of NADH oxidation could be only satisfactorily simulated by assuming both an initiation reaction between HNO_2 and NADH bound to LDH ($k = 520\ \text{M}^{-1}\text{s}^{-1}$, Table I, entry 12) and the subsequent propagation via $\text{O}_2^{\bullet-}$. Thus, as expected, HNO_2 obviously initiates an LDH-dependent chain oxidation of NADH similar to that observed with O_2 and H_2O_2 , respectively.

The NO_2^{\bullet} radical was generated from the NO^{\bullet} donating compound PAPA NONOate ($100\ \mu\text{M}$) and

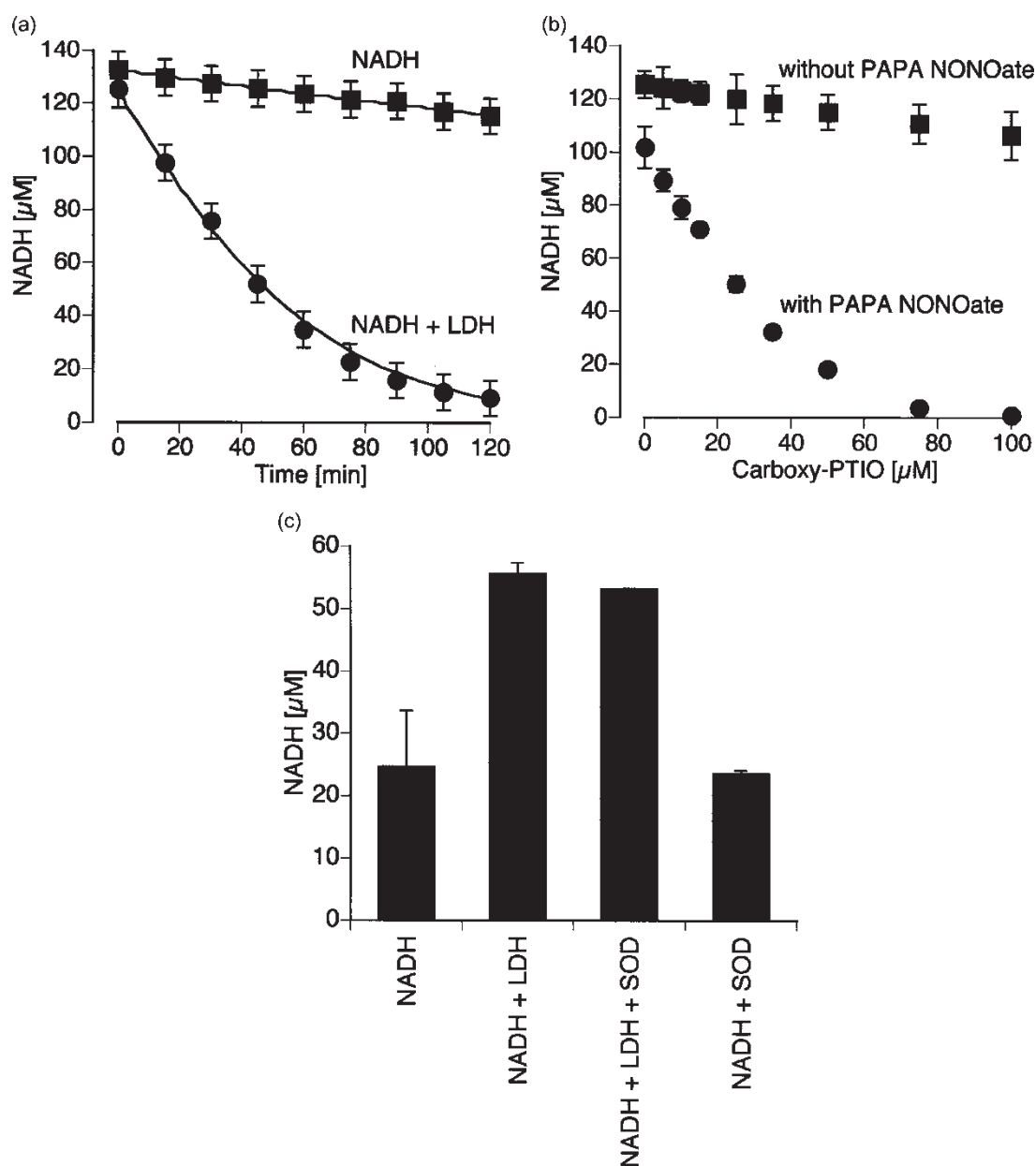


Figure 4. Effect of LDH on the oxidation of NADH by HNO_2 and NO_2^\bullet . If not stated otherwise, NADH (150 μM) was incubated in the absence and presence of lactate dehydrogenase (LDH, 10 μM) in phosphate buffer (50 mM, 25°C, pH 7.5) containing the transition metal chelator diethylenetriamine-pentaacetic acid (100 μM). (a), influence of LDH on the oxidation of NADH by HNO_2 as generated from nitrite (10 mM, added as NaNO_2 ; see reaction 5). These experiments were performed at pH 7.0 and 37°C in order to stimulate the formation of HNO_2 . (b), oxidation of free NADH by nitrogen dioxide (NO_2^\bullet) as generated from PAPA NONOate (100 μM) and carboxy-PTIO (5–100 μM) in Chelex 100-treated phosphate buffer. (c), influence of LDH on the oxidation of NADH by NO_2^\bullet as generated from 100 μM PAPA NONOate and 40 μM carboxy-PTIO; experimental conditions as in (b). The values shown in (b) and (c) were obtained 90 min after addition of the reactants. NADH oxidation was photometrically assessed from the decrease in absorption at 340 nm. Traces shown are means \pm S.D. of 2–8 independent experiments. The lines shown are the predictions of the kinetic simulations performed with the combined reaction set given in Ref. [18] and in Table I.

the NO^\bullet converter carboxy-PTIO (5–100 μM) [19]. In the absence of LDH, NADH oxidation strongly increased with increasing carboxy-PTIO concentrations, as to be expected (Figure 4b). Likewise, in the absence of PAPA NONOate, NADH was only slightly oxidized. In contrast to the initiating effect of HNO_2 , NADH oxidation by NO_2^\bullet was strongly diminished in the presence of LDH (10 μM , Figure 4c)

and LDH failed to mediate a superoxide-propagated chain radical reaction, as indicated by the inability of SOD to further decrease the NO_2^\bullet -mediated NADH oxidation (Figure 4c). Effective scavenging of NO_2^\bullet by LDH may also account for this behavior. Scavenging of NO_2^\bullet by LDH ($k = 1.3 \times 10^7 \text{ M}^{-1} \text{ s}^{-1}$, as estimated above) should lead to a decreased formation of the NAD^\bullet radical and, consequently, of $\text{O}_2^{\bullet-}$,

(reaction (2)). In addition, any remaining $O_2^{\bullet-}$ should be stoichiometrically trapped by NO_2^{\bullet} in a truly diffusion-controlled reaction to yield O_2NOO^- (see above). Thus, exclusively free NADH is oxidized by NO_2^{\bullet} and the remaining amounts of $O_2^{\bullet-}$ should be too low to effectively oxidize LDH-bound NADH via a chain radical mechanism. Due to the uncertainties of the chemical reactivities of the tyrosyl radicals at the surface and in the bulk of LDH, which would be formed after reaction with NO_2^{\bullet} (see above), but cannot be respected in our simulation reaction set, we refrained to perform a kinetic simulation here.

Discussion

An LDH-catalyzed chain oxidation of NADH can be initiated by various oxidants but is always propagated by $O_2^{\bullet-}$

In line with previous studies of Bielski and Chan reactions (1)–(4) [4–8], we here found that an LDH-catalyzed chain oxidation of NADH can be both initiated and propagated by $O_2^{\bullet-}$. However, in contrast to these former studies, we demonstrate that various oxidants other than $O_2^{\bullet-}$, i.e. O_2 , H_2O_2 , HNO_2 and authentic/*in situ* generated peroxy-nitrite, can initiate this chain oxidation of NADH, whereas the propagation is still and exclusively mediated by intermediary $O_2^{\bullet-}$. Weak (or moderately strong) oxidants (O_2 , H_2O_2 , HNO_2) were found to initiate the chain oxidation of NADH via slow reactions with LDH-bound NADH yielding NAD^{\bullet} , shown in Table I. In contrast, solely freely diffusing NADH is oxidized during the initiating reaction with strong oxidants (NO_2^{\bullet} , authentic/*in situ* generated peroxy-nitrite).

There are at least two reasons for the central and uniform role of $O_2^{\bullet-}$ in the subsequent propagation reactions: since the initiating oxidation of free and LDH-bound NADH always yields NAD^{\bullet} , $O_2^{\bullet-}$ is continuously formed and regenerated via one electron-transfer reduction of molecular oxygen at near to diffusion-controlled limit (reaction (2)). Besides this, the oxidation potential of the superoxide anion thus formed appears to be “optimal” to mediate the propagation cycle, i.e. on the one hand, $O_2^{\bullet-}$ seems not to react significantly with amino acid residues in LDH and hardly reacts with free NADH and NADPH, on the other hand, $O_2^{\bullet-}$ is apparently reactive enough to oxidize NADH bound to LDH.

The effect of LDH on the reactivity of NADH allowing the coenzyme to react with $O_2^{\bullet-}$ has not been satisfactorily clarified so far, although it was discovered already 30 years ago. We assume that binding to the coenzyme binding sites in the binary complex with LDH [23,27] increases the reductive power of NADH, which may be responsible not only for the transfer of hydrogen anions to pyruvate but also for

the increased reactivity towards $O_2^{\bullet-}$. In line with this, NADPH, which showed no binding interaction towards LDH, was not enabled to react with $O_2^{\bullet-}$. The concrete mechanism, however, underlying the effect of LDH on the reactivity of NADH, cannot be disclosed here.

Some of the (initiating) reactions presented here could not be extracted from experimental data and thus were exclusively evaluated with kinetical simulations. The use of large kinetic models (> 100 reactions) has the advantage to avoid the cancellation of unexpected but important reactions via a subjective selection process which is often called “chemical intuition”. A drawback of large kinetic models might be that the model is superfluous and/or redundant and that the importance of an individual reaction is unclear. Determining the importance of a reaction in a large kinetic model is the job of a sensitivity analysis and the various methods regarding this have been recently overviewed [21]. In the present work the reactions of interest were selected and ranked according to their importance with a sophisticated PCA [22] enacted on the NSCs. Due to the accurate “cut” of superfluous reactions, it was possible to describe the O_2 -/ H_2O_2 -dependent oxidation of NADH in the presence of LDH with 23 reactions and 18 reactions, respectively.

Strong oxidants oxidize free NADH and are scavenged by LDH

In contrast to the experiments with the weak oxidants, NADH consumption by strong oxidants could be satisfactorily simulated only in the absence of LDH. We attribute this failure to unknown reactions of the oxidants with the enzyme itself as indicated by the diminished NADPH oxidation in the presence of LDH. At the surface of LDH, a high number of prominent phenyl, tyrosyl and tryptophanyl residues is located, which appear to be possible targets for strong oxidants. These residues seem to be irrelevant for the catalytic behavior of the enzyme because their oxidation, as indicated by a decrease in the amino acid-dependent fluorescence of the enzyme, did not result in LDH inactivation (Petrat et al. unpublished results). Since Chan and Bielsky did not include controls with NADPH in their studies [4–9,40], a possible scavenging effect of LDH in reactions with HO_2^{\bullet} remained undetected.

The scavenging properties of the enzyme partly answer already the closely related question, why strong oxidants like NO_2^{\bullet} do not directly oxidize NADH bound to LDH, although it is more reactive than free NADH. Besides this, provided that nitrogen dioxide oxidizes indeed one NADH bound to LDH, superoxide would be formed (reaction (2)). However, as a consequence, a second NO_2^{\bullet} radical would be terminated in a diffusion-controlled reaction [41] by

the intermediately formed superoxide thereby preventing both the propagation of NADH oxidation by $O_2^{\bullet-}$ and the initiation reaction by a second nitrogen dioxide radical. Moreover, NADH bound to LDH is largely shielded by the enzyme as revealed from molecular models based on X-ray structure analysis of the coenzyme binding domain in LDH [42]. Therefore, reactions of strong oxidants with amino acid residues of the protein are more likely than their reaction with LDH-bound NADH.

Conclusions

As indicated by our experimental data and kinetic simulations, weak (or moderately strong) oxidants (O_2 , H_2O_2 , $O_2^{\bullet-}$, HNO_2) are capable of initiating a chain oxidation of LDH-bound NADH via slow direct reactions with the enzyme-bound coenzyme yielding H_2O_2 , NO^{\bullet} and/or 1–2 superoxide anion radicals per reaction cycle (see Table I). The superoxide then propagates the chain with very high efficacy (compare entries 5 and 3, 7, 12 in Table I) thereby restoring $O_2^{\bullet-}$ and generating H_2O_2 , i.e. an additional oxidant, so that the initially slow consumption of LDH-bound NADH by O_2 , H_2O_2 and HNO_2 is strongly amplified by intermediary $O_2^{\bullet-}$. Strong oxidants, which do not react directly with LDH-bound NADH, are exclusively scavenged by free NADH or by the enzyme itself and thus initiate the chain radical mechanism solely via intermediary $O_2^{\bullet-}$. These data demonstrate that the superoxide-dependent chain oxidation of LDH-bound NADH as introduced by Bielski and Chan [4–9] is of general importance because the chain mechanism can be initiated by a variety of oxidants. In this context, the continuous formation of $O_2^{\bullet-}$ and the additional generation of H_2O_2 may justify to characterize LDH-bound NADH as a prooxidant. In cellular systems, however, the LDH-catalyzed chain oxidation of NADH and thus the formation of reactive oxygen species should normally be effectively prevented by SOD (and catalase/glutathione peroxidase), being present at high concentrations in aerobic cells. This, on the other hand, further underlines the fundamental importance of SOD to terminate $O_2^{\bullet-}$ -dependent chain reactions and thus to prevent (amplification of) oxidative stress.

Acknowledgements

We would like to thank Ms Nicola Großebram for performing the experiment shown in Figure 4b, Dr H.-G. Korth (Institut für Organische Chemie, Universität Duisburg-Essen, Germany) for his critical comments to the manuscript, Dr J. C. Ianni for a series of clarifying discussions pertaining to the use of the new software package ATROPOS

and Ms Maren Holzhauser for her excellent technical assistance.

References

- [1] Wakita M, Nishimura G, Tamura M. Some characteristics of the fluorescence lifetime of reduced pyridine nucleotides in isolated mitochondria, isolated hepatocytes, and perfused rat liver *in situ*. *J Biochem* 1995;118:1151–1160.
- [2] Salmon J-M, Kohen E, Viallet P, Hirschberg JG, Wouters AW, Kohen C, Thorell B. Microspectrofluorometric approach to the study of free/bound NAD(P)H ratio as metabolic indicator in various cell types. *Photochem Photobiol* 1982;36:585–593.
- [3] Zewe V, Fromm HJ. Kinetic studies of rabbit muscle lactate dehydrogenase. *J Biol Chem* 1962;237:1668–1675.
- [4] Bielski BHJ, Chan PC. Enzyme-catalyzed free radical reactions with nicotinamide-adenine nucleotides. I. Lactate dehydrogenase-catalyzed chain oxidation of bound NADH by superoxide radicals. *Arch Biochem Biophys* 1973;159:873–879.
- [5] Bielski BHJ, Chan PC. Kinetic study by pulse radiolysis of the lactate dehydrogenase-catalyzed chain oxidation of nicotinamide adenine dinucleotide by HO_2 and $O_2^{\bullet-}$. *J Biol Chem* 1974;250:318–321.
- [6] Bielski BHJ, Chan PC. Re-evaluation of the kinetics of lactate dehydrogenase-catalyzed chain oxidation of nicotinamide adenine dinucleotide by superoxide radicals in the presence of ethylenediaminetetraacetate. *J Biol Chem* 1976; 251:3841–3844.
- [7] Chan PC, Bielski BHJ. Enzyme-catalyzed free radical reactions with nicotinamide adenine nucleotides. II. Lactate dehydrogenase-catalyzed oxidation of reduced nicotinamide adenine dinucleotide by superoxide radicals generated by xanthine oxidase. *J Biol Chem* 1974;249:1317–1319.
- [8] Chan PC, Bielski BHJ. Lactate dehydrogenase-catalyzed stereospecific hydrogen atom transfer from reduced nicotinamide adenine dinucleotide to dicarboxylate radicals. *J Biol Chem* 1975;250:7266–7271.
- [9] Chan PC, Bielski BHJ. Glyceraldehyde-3-phosphate dehydrogenase-catalyzed chain oxidation of reduced nicotinamide adenine dinucleotide by perhydroxyl radicals. *J Biol Chem* 1980;255:874–876.
- [10] Gutierrez-Correa J, Krauth-Siegel RL, Stoppani AOM. Phenothiazine radicals inactivate *Trypanosoma cruzi* dihydro-lipoamide dehydrogenase: Enzyme protection by radical scavengers. *Free Radic Res* 2003;37:281–291.
- [11] Kirsch M, de Groot H. NAD(P)H, a directly operating antioxidant? *FASEB J* 2001;15:1569–1574.
- [12] Petrat F, Pindiur S, Kirsch M, de Groot H. NAD(P)H, a primary target of 1O_2 in mitochondria of intact cells. *J Biol Chem* 2003;278:3298–3307.
- [13] Uppu RM, Pryor WA. Synthesis of peroxynitrite in a two-phase system using isoamyl nitrite and hydrogen peroxide. *Anal Biochem* 1996;236:242–249.
- [14] Velick SF, Hayes JE, Harting J. The binding of diphosphopyridine nucleotide by glyceraldehyde-3-phosphate dehydrogenase. *J Biol Chem* 1953;203:527–544.
- [15] Bergmeyer HU. Methods of enzymatic analysis. Samples, reagents, assessment of results. Weinheim: VCH Verlagsgesellschaft; 1986.
- [16] Kirsch M, Lomonosova EE, Korth H-G, Sustmann R, de Groot H. Hydrogen peroxide formation by reaction of peroxynitrite with HEPES and related tertiary amines. Implications for a general mechanism. *J Biol Chem* 1998; 273:12716–12724.
- [17] Wolfe SK, Swinehart HJ. Photochemistry of pentacyanonitrosylferrate(2-), nitroprusside. *Inorg Chem* 1975;14:1049–1053.
- [18] Kirsch M, Korth H-G, Wensing A, Sustmann R, de Groot H. Product formation and kinetic simulations in the pH range 1–14 account for a free-radical mechanism of peroxynitrite decomposition. *Arch Biochem Biophys* 2003;418:133–150.

- [19] Goldstein S, Russo A, Samuni A. Reactions of PTIO and Carboxy-PTIO with NO^\bullet , NO_2^\bullet , and O_3^\bullet . *J Biol Chem* 2003; 278:50949–50955.
- [20] Evans PJ, Halliwell B. Measurement of iron and copper in biological systems: Bleomycin and copper-phenanthroline assays. *Methods Enzymol* 1994;233:82–92.
- [21] Saltelli A, Ratto M, Tarantola S, Campolongo F. Sensitivity analysis for chemical models. *Chem Rev* 2005; ASAP Article; DOI: 10.1021/cr040659d.
- [22] Vajda S, Valko P, Turanyi T. Principal component analysis of kinetic models. *Int J Chem Kinet* 1985;17:55–81.
- [23] Branden CI, Eklund H. Structure and mechanism of liver alcohol dehydrogenase, lactate dehydrogenase and glyceraldehyde-3-phosphate dehydrogenase. In: Jeffery J, editor. *Experientia-supplementum*. Basel: Birkhäuser; 1980. p 40–84.
- [24] Winer AD, Schwert GW. Lactic dehydrogenase: Fluorescence spectra of ternary complexes of lactic dehydrogenase, reduced diphosphopyridine nucleotide, and carboxylic acids. *J Biol Chem* 1959;234:1155–1161.
- [25] Winer AD, Schwert GW, Millar DBS. Lactic dehydrogenase: Fluorimetric measurements of the complex of enzyme and reduced diphosphopyridine nucleotide. *J Biol Chem* 1959; 234:1149–1154.
- [26] Fischer HF, McGregor LL. The nature of the fluorescence of an enzyme-reduced coenzyme-reduced substrate complex. *Biochim Biophys Acta* 1960;43:556–557.
- [27] Deng H, Zhadin N, Callender R. Dynamics of protein ligand binding on multiple time scales: NADH binding to lactate dehydrogenase. *Biochemistry* 2001;40:3767–3773.
- [28] Bernofsky C, Wanda S-YC. Formation of reduced nicotinamide adenine dinucleotide peroxide. *J Biol Chem* 1982; 257:6809–6817.
- [29] Petrat F, Paluch S, Dogruöz E, Dörfler P, Kirsch M, Korth HG, Sustmann R, de Groot H. Reduction of iron(III) ions complexed to physiological ligands by lipoyl dehydrogenase and other flavoenzymes *in vitro*. Implications for an enzymatic reduction of Fe(III) ions of the labile iron pool. *J Biol Chem* 2003;278:46403–46413.
- [30] Swintek AU, Christoph S, Petrat F, de Groot H, Kirsch M. Cell type-dependent release of nitric oxide and/or reactive nitrogenoxide species from intracellular SIN-1: Effects on cellular NAD(P)H. *Biol Chem* 2004;385:639–648.
- [31] Garcia-Nogales P, Almeida A, Bolaños JP. Peroxynitrite protects neurons against nitric oxide-mediated apoptosis. A key role for glucose-6-phosphate dehydrogenase activity in neuroprotection. *J Biol Chem* 2003;278:864–874.
- [32] Lomonosova E, Kirsch M, Rauen U, de Groot H. The critical role of Hepes in SIN-1 cytotoxicity, peroxynitrite versus hydrogen peroxide. *Free Radic Biol Med* 1998;24:522–552.
- [33] Schönafinger K. Heterocyclic NO prodrugs. *Il Farmaco* 1999; 54:316–320.
- [34] Ross AB, Mallard WG, Helman WP, Buxton GV, Huie RE, Neta P. NDRL/NIST solution kinetics database 3.0. Gaithersburg, MD: 1998.
- [35] Goldstein S, Czapski G. Reactivity of peroxynitrite versus simultaneous generation of NO^\bullet and $\text{O}_2^{\bullet-}$ toward NADH. *Chem Res Toxicol* 2000;13:736–741.
- [36] Kirsch M, de Groot H. Reaction of peroxynitrite with reduced nicotinamide nucleotides, formation of hydrogen peroxide. *J Biol Chem* 1999;274:24664–24670.
- [37] Kirsch M, de Groot H. Ascorbate is a potent antioxidant against peroxynitrite-induced oxidation reactions. *J Biol Chem* 2000;275:16702–16708.
- [38] Berman HM, Westbrook J, Feng Z, Gilliland G, Bhat TN, Weissig H, Shindyalov IN, Bourne PE. The protein data bank. *Nucleic Acids Res* 2000;28:235–242.
- [39] Prütz WA, Mönig H, Butler J, Land EJ. Reactions of nitrogen dioxide in aqueous model systems: Oxidation of tyrosine units in peptides and proteins. *Arch Biochem Biophys* 1985;243:125–134.
- [40] Bielski BHJ, Cabelli DE, Arudi RL, Ross AB. Reactivity of HO_2^\bullet radicals in aqueous solution. *J Phys Chem Ref Data* 1985;14:1041–1062.
- [41] Kirsch M, Korth H-G, Sustmann R, de Groot H. The pathobiochemistry of nitrogen dioxide. *Biol Chem* 2002; 383:389–399.
- [42] Buehner M. The architecture of the coenzyme binding domain in dehydrogenases as revealed by X-ray structure analysis. *Dehydrogenase Symposium*. Konstanz, Germany: 1974. p 78.
- [43] Scheeline A, Olson DL, Williksen EP, Horras GA. The peroxidase-oxidase oscillator and its constituent chemistries. *Chem Rev* 1997;97:739–756.
- [44] Lvovich V, Scheeline A. Complexation of nicotinamide adenine dinucleotide with ferric and ferrous ions. *Arch Biochem Biophys* 1995;320:1–13.
- [45] Land EJ, Swallow AJ. One-electron reactions in biochemical systems as studied by pulse radiolysis. IV. Oxidation of dihydronicotinamide-adenine dinucleotide. *Biochim Biophys Acta* 1971;234:34–42.
- [46] Goldstein S, Czapski G. Reactivity of peroxynitric acid (O_2NOOH): A pulse radiolysis study. *Inorg Chem* 1997;36: 4156–4162.

Appendix

Table IS. Influential reactions for the decay of 150 μM NADH in the presence of both 10 μM LDH and 225 μM O_2 at pH 7.0 according to the principal component analysis of the normalized sensitivity coefficients derived from calculations performed with Kintecus and Atropos, respectively.

No	Entry in Table 1	Reaction	Rate constant*	B_r^\dagger
1	3	$\text{LDH-NADH} + \text{O}_2 \rightarrow \text{LDH-NAD}^\bullet + \text{HOO}^\bullet$	1.6×10^{-4}	349.6
2	7	$\text{LDH-NADH} + \text{H}_2\text{O}_2 \rightarrow \text{LDH-NAD}^\bullet + \text{H}_2\text{O} + \text{HO}^\bullet$	2.0×10^{-4}	276.1
3	5	$\text{LDH-NADH} + \text{O}_2^{\bullet-} \rightarrow \text{LDH-NAD}^\bullet + \text{HOO}^-$	3.6×10^4	264.4
4	19	$\text{LDH-NAD}^\bullet + \text{O}_2 \rightarrow \text{LDH-NAD}^+ + \text{O}_2^{\bullet-}$	3.2×10^9	250.3
5		$\text{H}_2\text{O}_2 + \text{HO}^\bullet \rightarrow \text{HOO}^\bullet + \text{H}_2\text{O}$	2.7×10^7	245.1
6		$\text{O}_2^{\bullet-} + \text{H}_3\text{O}^+ \rightarrow \text{HOO}^\bullet + \text{H}_2\text{O}$	5.0×10^{10}	150.1
7		$\text{HOO}^\bullet + \text{H}_2\text{O} \rightarrow \text{O}_2^{\bullet-} + \text{H}_3\text{O}^+$	1.4×10^4	129.9
8		$\text{O}_2^{\bullet-} + \text{HOO}^\bullet \rightarrow \text{HOO}^- + \text{O}_2$	9.7×10^7	98.8
9	14	$\text{LDH} + \text{NADH} \rightarrow \text{LDH-NADH}$	1.0×10^6	76.9
10	15	$\text{LDH-NADH} \rightarrow \text{LDH} + \text{NADH}$	1.0×10^1	66.9
11		$\text{HOO}^- + \text{H}_3\text{O}^+ \rightarrow \text{H}_2\text{O}_2 + \text{H}_2\text{O}$	5.0×10^{10}	50.3
12	20	$2\text{NAD}^\bullet \rightarrow (\text{NAD})_2$	5.6×10^7	50.0
13	2	$\text{NADH} + \text{H}_3\text{O}^+ \rightarrow \text{HNADH}^+ + \text{H}_2\text{O}$	7	49.9
14	8	$\text{NADH} + \text{HOO}^\bullet \rightarrow \text{NAD}^\bullet + \text{H}_2\text{O}_2$	1.8×10^5	49.3
15		$\text{H}_2\text{O}_2 + \text{H}_2\text{O} \rightarrow \text{HOO}^- + \text{H}_3\text{O}^+$	3.2×10^{-3}	48.7
16	18	$\text{NAD}^\bullet + \text{O}_2 \rightarrow \text{NAD}^+ + \text{O}_2^{\bullet-}$	2.0×10^9	45.2
17	17	$\text{LDH-NAD}^+ \rightarrow \text{LDH} + \text{NAD}^+$	1.5×10^2	44.6
18	16	$\text{LDH} + \text{NAD}^+ \rightarrow \text{LDH-NAD}^+$	1.0×10^6	44.4
19	1	$\text{NADH} + \text{O}_2 \rightarrow \text{NAD}^+ + \text{HOO}^-$	1.8×10^{-10}	17.1
20		$\text{HO}^\bullet + \text{O}_2^{\bullet-} \rightarrow \text{O}_2 + \text{HO}^-$	1.1×10^{10}	15.3
21	9	$\text{LDH-NADH} + \text{HOO}^\bullet \rightarrow \text{LDH-NAD}^\bullet + \text{H}_2\text{O}_2$	2.0×10^6	8.8
22		$\text{HOO}^- + \text{HO}^\bullet \rightarrow \text{HOO}^\bullet + \text{HO}^-$	7.5×10^9	7.0
23		$2\text{HO}^\bullet \rightarrow \text{H}_2\text{O}_2$	5.5×10^9	6.6

* In s^{-1} , $\text{M}^{-1} \text{s}^{-1}$, or $\text{M}^{-2} \text{s}^{-1}$; pseudo-order rate constants of reactions involving water were divided by $[\text{H}_2\text{O}]_0 = 55.56 \text{ M}$. $^\dagger B_r$ = overall squared sensitivity coefficient.

Table IIS. Influential reactions for the decay of 150 μM NADH in the presence of both 10 μM LDH, 600 μM H_2O_2 and 225 μM O_2 at pH 7.0 according to the principal component analysis of the normalized sensitivity coefficients derived from calculations performed with Kintecus and Atropos, respectively.

No	Entry in Table 1	Reaction	Rate constant*	B_r^\dagger
1	7	$\text{LDH-NADH} + \text{H}_2\text{O}_2 \rightarrow \text{LDH-NAD}^\bullet + \text{H}_2\text{O} + \text{HO}^\bullet$	2.0×10^{-4}	420.9
2		$\text{H}_2\text{O}_2 + \text{HO}^\bullet \rightarrow \text{HOO}^\bullet + \text{H}_2\text{O}$	2.7×10^7	344.6
3	19	$\text{LDH-NAD}^\bullet + \text{O}_2 \rightarrow \text{LDH-NAD}^+ + \text{O}_2^{\bullet-}$	3.2×10^9	252.3
4	5	$\text{LDH-NADH} + \text{O}_2^{\bullet-} \rightarrow \text{LDH-NAD}^\bullet + \text{HOO}^-$	3.6×10^4	246.9
5		$\text{HOO}^\bullet + \text{H}_2\text{O} \rightarrow \text{O}_2^{\bullet-} + \text{H}_3\text{O}^+$	1.4×10^4	117.2
6		$\text{O}_2^{\bullet-} + \text{H}_3\text{O}^+ \rightarrow \text{HOO}^\bullet + \text{H}_2\text{O}$	5.0×10^{10}	116.8
7		$\text{O}_2^{\bullet-} + \text{HOO}^\bullet \rightarrow \text{HOO}^- + \text{O}_2$	9.7×10^7	98.4
8	8	$\text{NADH} + \text{HOO}^\bullet \rightarrow \text{NAD}^\bullet + \text{H}_2\text{O}_2$	1.8×10^5	86.4
9	14	$\text{LDH} + \text{NADH} \rightarrow \text{LDH-NADH}$	1.0×10^6	61.1
10	15	$\text{LDH-NADH} \rightarrow \text{LDH} + \text{NADH}$	1.0×10^1	61.0
11	18	$\text{NAD}^\bullet + \text{O}_2 \rightarrow \text{NAD}^+ + \text{O}_2^{\bullet-}$	2.0×10^9	52.3
12		$\text{HOO}^- + \text{H}_3\text{O}^+ \rightarrow \text{H}_2\text{O}_2 + \text{H}_2\text{O}$	5.0×10^{10}	50.3
13		$\text{H}_2\text{O}_2 + \text{H}_2\text{O} \rightarrow \text{HOO}^- + \text{H}_3\text{O}^+$	3.2×10^{-3}	50.0
14	2	$\text{NADH} + \text{H}_3\text{O}^+ \rightarrow \text{HNADH}^+ + \text{H}_2\text{O}$	7	49.9
15	17	$\text{LDH-NAD}^+ \rightarrow \text{LDH} + \text{NAD}^+$	1.5×10^2	42.6
16	9	$\text{LDH-NADH} + \text{HOO}^\bullet \rightarrow \text{LDH-NAD}^\bullet + \text{H}_2\text{O}_2$	2.0×10^6	7.1
17	3	$\text{LDH-NADH} + \text{O}_2 \rightarrow \text{LDH-NAD}^\bullet + \text{HOO}^\bullet$	1.6×10^{-4}	7.0
18	1	$\text{NADH} + \text{O}_2 \rightarrow \text{NAD}^+ + \text{HOO}^-$	1.8×10^{-10}	2.2

* In s^{-1} , $\text{M}^{-1} \text{s}^{-1}$, or $\text{M}^{-2} \text{s}^{-1}$; pseudo-order rate constants of reactions involving water were divided by $[\text{H}_2\text{O}]_0 = 55.56 \text{ M}$. $^\dagger B_r$ = overall squared sensitivity coefficient.

Table III. Influential reactions for the peroxynitrite-dependent (100 μM) oxidation of 150 μM NADH in the presence of 225 μM O_2 at pH 7.5 according to the principal component analysis of the normalized sensitivity coefficients derived from calculations performed with Kintecus and Atropos, respectively.

No	Entry in Table I	Reaction	Rate constant*	B_r^\dagger
1		$\text{ONOO}^- + \text{H}_3\text{O}^+ \rightarrow \text{ONOOH} + \text{H}_2\text{O}$	5×10^{10}	49488.3
2		$\text{ONOOH} + \text{H}_2\text{O} \rightarrow \text{ONOO}^- + \text{H}_3\text{O}^+$	143	46205.6
3		$\text{ONOOH} \rightarrow \text{HNO}_3$	0.94	17982.8
4	10	$\text{NADH} + \text{ONOOH} \rightarrow \text{H}_2\text{O} + \text{NAD}^\bullet + \text{H}_3\text{O}^+ + \text{NO}_2^\bullet$	7.4×10^3	6514.3
5		$\text{HNO}_2 + \text{H}_2\text{O} \rightarrow \text{H}_3\text{O}^+ + \text{NO}_2^\bullet$	7.2×10^5	2745.4
6		$\text{H}_3\text{O}^+ + \text{NO}_2^\bullet \rightarrow \text{HNO}_2 + \text{H}_2\text{O}$	5×10^{10}	2713.2
7		$\text{ONOOH} \rightarrow \text{HO}^\bullet + \text{NO}_2^\bullet$	0.36	2274.7
8	13	$\text{NADH} + \text{NO}_2^\bullet \rightarrow \text{NAD}^\bullet + \text{HNO}_2$	4.0×10^3	894.7
9		$2 \text{HNO}_2 \rightarrow \text{N}_2\text{O}_3 + \text{H}_2\text{O}$	13.4	632.4
10		$\text{O}_2\text{NOO}^- \rightarrow \text{NO}_2^- + \text{O}_2$	1.4	487.6
11		$\text{NAD}^\bullet + \text{O}_2 \rightarrow \text{NAD}^+ + \text{O}_2^{\bullet-}$	2.0×10^9	403.6
12		$\text{HO}^\bullet + \text{NO}_2^- \rightarrow \text{HO}^- + \text{NO}_2^\bullet$	5.3×10^9	352.8
13		$\text{O}_2^{\bullet-} + \text{NO}_2^\bullet \rightarrow \text{O}_2\text{NOO}^-$	4.5×10^9	322.3
14		$\text{O}_2^{\bullet-} + \text{H}_2\text{O} \rightarrow \text{HO}^\bullet + \text{HO}^-$	1.7×10^6	321.1
15		$\text{HO}^\bullet + \text{HO}^- \rightarrow \text{O}^{\bullet-} + \text{H}_2\text{O}$	1.3×10^{10}	318.4
16		$\text{O}_2\text{NOOH} + \text{H}_2\text{O} \rightarrow \text{O}_2\text{NOO}^- + \text{H}_3\text{O}^+$	1.43×10^3	220.2
17		$\text{H}_3\text{O}^+ + \text{O}_2\text{NOO}^- \rightarrow \text{O}_2\text{NOOH} + \text{H}_2\text{O}$	5×10^{10}	215.3
18		$\text{O}^{\bullet-} + \text{O}_2 \rightarrow \text{O}_2^{\bullet-}$	3.8×10^9	159.8
19		$\text{NADH} + \text{O}_2\text{NOOH} \rightarrow \text{NO}_2^\bullet + \text{NAD}^+ + \text{H}_2\text{O}_2$	1.0×10^4	140.9
20	11	$\text{O}_3^{\bullet-} \rightarrow \text{O}^{\bullet-} + \text{O}_2$	4×10^3	136.3
21		$\text{N}_2\text{O}_3 \rightarrow \text{NO}^\bullet + \text{NO}_2^\bullet$	8.0×10^4	131.0
22		$\text{HOO}^\bullet + \text{H}_2\text{O} \rightarrow \text{O}_2^{\bullet-} + \text{H}_3\text{O}^+$	1.4×10^4	129.9
23		$\text{O}_2^{\bullet-} + \text{H}_3\text{O}^+ \rightarrow \text{HOO}^\bullet + \text{H}_2\text{O}$	5×10^{10}	129.2
24		$\text{N}_2\text{O}_3 + \text{H}_2\text{O} (+\text{HPO}_4^{2-}) \rightarrow 2 \text{HNO}_2$	$2 \times 10^3 + 8 \times 10^5 \times [\text{HPO}_4^{2-}]$	120.7
25		$\text{ONOO}^- + \text{HO}^\bullet \rightarrow \text{HO}^- + \text{NO}^\bullet + \text{O}_2$	4.8×10^9	117.9
26		$\text{O}_2^{\bullet-} + \text{NO}^\bullet \rightarrow \text{ONOO}^-$	6.7×10^9	95.6
27		$\text{NO}_2^\bullet + 2 \text{H}_2\text{O} \rightarrow \text{HNO}_3 + \text{H}_3\text{O}^+$	9×10^6	86.7
28		$\text{HNO}_3 + \text{H}_2\text{O} \rightarrow \text{NO}_3^- + \text{H}_3\text{O}^+$	2.0×10^{10}	80.4
29		$\text{HOO}^- + \text{H}_3\text{O}^+ \rightarrow \text{H}_2\text{O}_2 + \text{H}_2\text{O}$	5×10^{10}	80.4
30		$\text{NO}_3^{\bullet-} + \text{H}_2\text{O} \rightarrow \text{NO}_2^\bullet + 2 \text{HO}^-$	1×10^3	80.2
31		$\text{ONOOH} + \text{H}_3\text{O}^+ \rightarrow \text{NO}_2^\bullet + 2 \text{H}_2\text{O}$	6.22	80.0
32	20	$2 \text{NAD}^\bullet \rightarrow (\text{NAD})_2$	2.0×10^9	80.0
33		$\text{HO}^\bullet + \text{O}_3^{\bullet-} \rightarrow \text{HO}^- + \text{O}_3$	8.5×10^9	80.0
34	2	$\text{NADH} + \text{H}_3\text{O}^+ \rightarrow \text{HNADH}^+ + \text{H}_2\text{O}$	7	80.0
35		$\text{NO}_3^- + \text{H}_3\text{O}^+ \rightarrow \text{HNO}_3 + \text{H}_2\text{O}$	5×10^{10}	80.0
36		$\text{O}^{\bullet-} + \text{NO}_2^\bullet \rightarrow \text{NO}_3^{\bullet-}$	1.8×10^7	79.8
37		$\text{O}_2\text{NOO}^- \rightarrow \text{O}_2^{\bullet-} + \text{NO}_2^\bullet$	1.05	79.6
38		$\text{H}_2\text{O}_2 + \text{H}_2\text{O} \rightarrow \text{HOO}^- + \text{H}_3\text{O}^+$	3.2×10^{-3}	79.4
39		$2 \text{NO}_2^\bullet \rightarrow \text{N}_2\text{O}_4$	4.5×10^8	69.0
40		$\text{N}_2\text{O}_4 \rightarrow 2 \text{NO}_2^\bullet$	6.9×10^3	56.1

TABLE III S - continued

No	Entry in Table I	Reaction	Rate constant*	B_t^\dagger
41	8	$\text{NADH} + \text{HOO}^\bullet \rightarrow \text{NAD}^\bullet + \text{H}_2\text{O}_2$	1.8×10^5	51.5
42		$\text{ONOO}^- \rightarrow \text{O}^\bullet + \text{NO}_2^\bullet$	1.7×10^{-6}	40.1
43		$\text{N}_2\text{O}_4(+\text{H}_2\text{O}) \rightarrow \text{HNO}_2 + \text{HNO}_3$	18	35.9
44		$\text{NO}^\bullet + \text{NO}_2^\bullet \rightarrow \text{N}_2\text{O}_3$	1.1×10^9	25.1

* In s^{-1} , $\text{M}^{-1} \text{s}^{-1}$, or $\text{M}^{-2} \text{s}^{-1}$; pseudo-order rate constants of reactions involving water were divided by $[\text{H}_2\text{O}]_0 = 55.56 \text{ M}$. $^\dagger B_t =$ overall squared sensitivity coefficient.